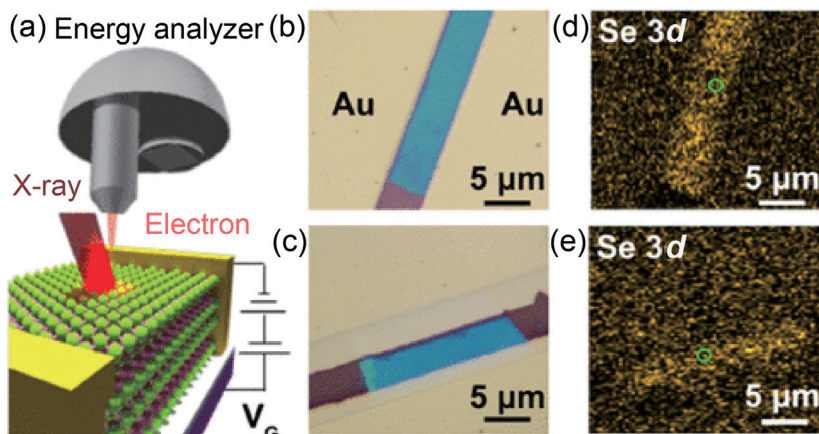


In–O and In–Se signals varied from 1.91 eV ( $V_G = 0$  V) to 1.45 eV ( $V_G = 50$  V). This decrease in the relative energy difference under the application of a 50-V  $V_G$  indicates that compared with  $V_G = 0$  V, photoemitted electrons from oxidation sites are accelerated by the external electric field, resulting in a red shift of the binding energy. Note that, during the measurements, the InSe channel was grounded to an energy analyzer, and if there were no charge accumulation on the sample surface, there would be no potential difference between the energy analyzer and InSe due to the alignment of the Fermi level. Based on this assumption, they inferred that the external electric field was ascribed to the accumulation of induced electrons at the surface oxidation sites, producing an electrostatic potential on the InSe surface layer.

In summary, the demonstrated characteristics indicate that the engineering of an InSe interface has potential applications for nonvolatile memory. (Reported by Cheng-Maw Cheng)

*This report features the work of Yi-Ying Lu, Chia-Hao Chen and their collaborators published in ACS Appl. Mater. Interfaces* **13**, 4618 (2021).



**Fig. 1:** Operando scanning photoelectron microscopic characterization of van der Waals gate devices. (a) Schematic of the operando SPEM measurement setup. (b,c) Optical images of pristine (top) and oxygen-plasma-treated devices (bottom). (d,e) Photoelectron intensity mapping of the Se 3d core-level spectra of pristine (top) and oxygen plasma-treated devices (bottom). [Reproduced from Ref. 1]

#### TLS 09A1 SPEM

- XPS, AES, photoabsorption, and other spectra
- Materials Science, Condensed-matter Physics

#### Reference

1. Y.-Y. Lu, Y.-T. Peng, Y.-T. Huang, J.-N. Chen, J. Zhou, L.-W. Lan, S.-H. Jian, C.-C. Kuo, S.-H. Hsieh, C.-H. Chen, R. Sanakar, F.-C. Chou, *ACS Appl. Mater. Interfaces* **13**, 4618 (2021).

## A Double Perovskite Oxide Shows the Way for High Performance of Electrocatalytic Water Oxidation

*In-situ/operando X-ray absorption spectra of double perovskite  $Sr_2CoIrO_{6-\delta}$  identify the role of an uncommon hexavalent  $Ir^{6+}$  configuration in accelerating electrocatalytic water oxidation.*

A main goal of the recently held UN Climate Change Conference was to secure global net-zero emissions of carbon dioxide by 2050. To achieve this goal, countries must phase out the use of coal, decrease deforestation, speed up switching to electric vehicles and increase renewable energy sources. The challenge of improved renewable energy technologies is thus an important part of saving our planet from severe climate change. Identifying materials that are efficient electrochemical catalysts is a major requirement of renewable energy technologies.

Further, to develop such materials, it is necessary to understand the mechanism of the oxygen-evolution reaction (OER) that exhibits sluggish reaction kinetics, and find ways to improve its efficiency. Oxygen evolution is the process of generating molecular oxygen ( $O_2$ ) by a chemical reaction, generally from water, and occurs in photosynthesis, electrolysis of water and decomposition of oxides.

In a recent report in *Advanced Functional Materials*,<sup>1</sup>

researchers showed that a double perovskite oxide compound  $\text{Sr}_2\text{CoIrO}_{6-6}$  exhibits an unprecedentedly small overpotential of 210 mV to achieve a current density of  $10 \text{ mA cm}^{-2}$ . This result makes  $\text{Sr}_2\text{CoIrO}_{6-6}$  the most efficient perovskite-based solid-state catalyst for OER. The authors carried out an extensive set of measurements on polycrystalline  $\text{Sr}_2\text{CoIrO}_{6-6}$  to identify the real active sites and to understand the mechanism of OER. Polycrystalline samples of  $\text{Sr}_2\text{CoIrO}_{6-6}$  were synthesized with a solid-state reaction method. The crystal structure and morphology

were investigated with X-ray diffraction and a transmission electron microscope to prove that approximately 90% of the Co/Ir ions were ordered on alternate sites in three dimensions of the double perovskite structure. Linear sweep voltammetry was implemented to quantify the OER activity of the electrocatalysts; the results showed an activity order of  $\text{Sr}_2\text{CoIrO}_{6-6} > \text{IrO}_2 > \text{SrIrO}_{3-6} > \text{SrCoO}_{3-6}$ . It was further shown that  $\text{Sr}_2\text{CoIrO}_{6-6}$  exhibited an iridium mass activity  $0.84 \text{ A mg}^{-1}_{\text{Ir}}$ , which was approximately 7.0 and 5.6 times that of  $\text{SrCoO}_{3-6}$  ( $0.12 \text{ A mg}^{-1}_{\text{Ir}}$ ) and  $\text{IrO}_2$

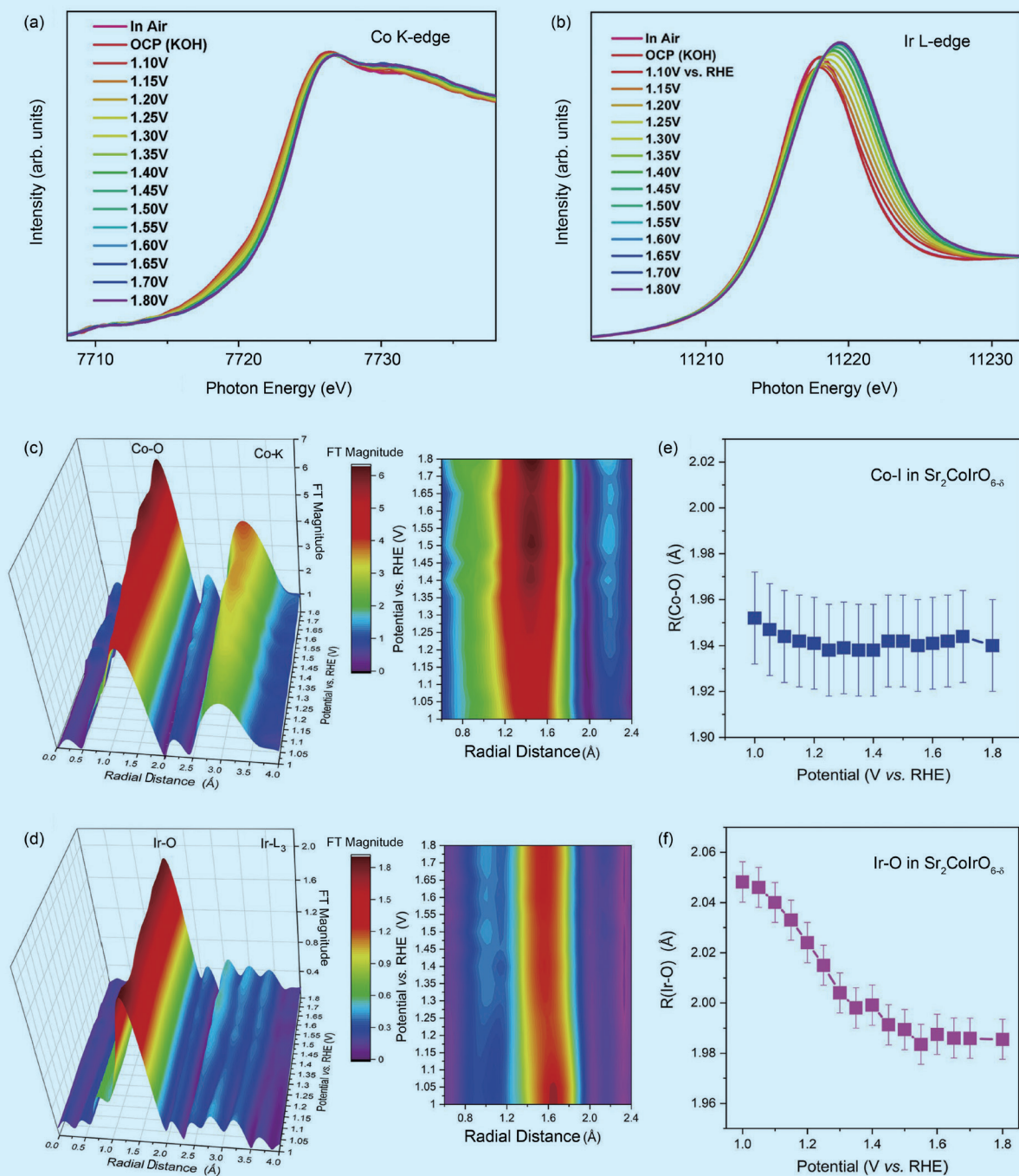


**Fig. 1:** Rapid *operando* spectral characterizations. (a,b) Co-K edge and Ir-L<sub>3</sub> edge XANES spectra of  $\text{Sr}_2\text{CoIrO}_{6-6}$  electrocatalyst at varied applied voltage. (c,d) 3D *operando* Fourier transforms of EXAFS spectra at (c) Co-K edge and (d) Ir-L<sub>3</sub> edge as a function of applied potential, with corresponding enlarged-scale 2D contour plots of the Co-O and Ir-O ranges. The EXAFS data are not corrected for phase shift. (e,f) Co-O and Ir-O bond lengths in  $\text{Sr}_2\text{CoIrO}_{6-6}$  electrocatalyst under applied potential extracted from EXAFS fitting. The applied voltage is referred to the reversible hydrogen electrode. [Reproduced from Ref. 1]

(0.15 A mg<sup>-1</sup><sub>Ir</sub>), respectively. Sr<sub>2</sub>CoIrO<sub>6-δ</sub> possessed the smallest Tafel slope (54 mV dec<sup>-1</sup>), indicating that it had the best reaction kinetics of all other Co- and Ir-containing control electrocatalysts.

More importantly, using rapid *operando* X-ray absorption near-edge spectroscopy (XANES) measured at **TPS 44A**,<sup>1</sup> the true active sites and the evolution of their valence states in Sr<sub>2</sub>CoIrO<sub>6-δ</sub> were examined at the Co-K and Ir-L<sub>3</sub> edges during the OER. It is well known that XANES spectra at the 3d element K edge are highly sensitive to the valence state: an increased valence state of the metal ion by one unit typically causes an energy shift of the absorption edge by more than 1 eV (e.g. 2.3 eV from Co<sup>2+</sup> to Co<sup>3+</sup> and 1.5 eV from Co<sup>3+</sup> to Co<sup>4+</sup>). **Figure 1(a)** shows the *operando* Co-K XANES spectra of the Sr<sub>2</sub>CoIrO<sub>6-δ</sub> catalyst under OER. The pristine Sr<sub>2</sub>CoIrO<sub>6-δ</sub> shows Co ions in Co<sup>3+</sup> state in the Co K-edge XANES spectrum, which was also confirmed by Co L-edge soft X-ray absorption spectra measured at **TLS 11A1**. Upon increasing the applied voltage, the Co-K XANES spectra of Sr<sub>2</sub>CoIrO<sub>6-δ</sub> gradually shifted to increased energies up to 0.5 eV at 1.8 V. This effect indicates a transition from Co<sup>3+</sup> state to Co<sup>4+</sup> state in Sr<sub>2</sub>CoIrO<sub>6-δ</sub>. Compared with the Co<sup>3+</sup> and Co<sup>4+</sup> reference materials EuCo<sup>3+</sup>O<sub>3</sub> and BaCo<sup>4+</sup>O<sub>3</sub>, the average Co valence state of Sr<sub>2</sub>CoIrO<sub>6-δ</sub> was estimated to be +3.3 at 1.8 V, and nearly +3.4 in SrCoO<sub>2.7</sub>. Similarly, the XANES Ir-L<sub>3</sub> edge spectra of Sr<sub>2</sub>CoIrO<sub>6-δ</sub> were recorded as a function of applied voltage as shown in **Fig. 1(b)**, and compared with spectra of Ir reference materials SrlrO<sub>3</sub> for Ir<sup>4+</sup>, stoichiometric Sr<sub>2</sub>CoIrO<sub>6-δ</sub> for Ir<sup>5+</sup>, and Sr<sub>2</sub>CoIrO<sub>6</sub> for Ir<sup>6+</sup>. The authors then established that the Ir-L<sub>3</sub> edge significantly shifted to higher energy with increasing applied potential up to 1.8 eV, indicating a valency increase from Ir<sup>4+</sup> to Ir<sup>5+</sup>, and further increased to the highest valence state of Ir<sup>6+</sup> under OER conditions. The estimated average valence state of Ir was +5.4 at 1.8 V. The authors thus proved that *operando* Co-K and Ir-L<sub>3</sub> XANES spectra showed that both Co and Ir ions are OER-active sites in Sr<sub>2</sub>CoIrO<sub>6-δ</sub>. This is the first observation of such a high valence state of Ir<sup>6+</sup> under OER condition.

Further, the authors studied the local coordination of the OER-active Co and Ir ions using *operando* extended X-ray absorption fine structure (EXAFS) spectra. 3D Fourier-transform patterns of the Co-K and Ir-L<sub>3</sub> edge spectra as a function of applied potential appear in **Figs. 1(c) and 1(d)**; the evolution of Co-O and Ir-O bond lengths was obtained from fitting the EXAFS, as shown in **Figs. 1(e) and 1(f)**. The Co-O bond length was found to decrease only slightly with

increasing applied voltage (**Fig. 1(e)**), but the Ir-O bond length showed a gradual decrease from 2.048(7) Å at 1.0 V to 1.984(8) Å at 1.55 V and became nearly constant for 1.6–1.8 V (**Fig. 1(f)**). Using a known relation<sup>2</sup> between Ir-O bond distance and the corresponding Ir oxidation state that showed the Ir-O bond length decreases by 0.039 Å per oxidation state, the Ir oxidation state under *operando* condition was independently estimated from ≈5 at 1.4 V to ≈5.4 for 1.6–1.8 V. This result is consistent with the oxidation state obtained from the white line shift of the XANES analysis and supports the presence of a high valence state of Ir<sup>6+</sup> under OER conditions.

To understand the origin of the ultrahigh OER in the Sr<sub>2</sub>CoIrO<sub>6-δ</sub> system, the authors made calculations with density-functional theory (DFT). They employed supercell calculations of SrCoO<sub>3-δ</sub> embedded with Ir to show that the electron density surrounding the Ir-O-Co path increases with respect to the Co-O-Co path. This effect indicates stronger bonding between Ir/Co 5d/3d and O 2p states, thereby supporting the important role of 5d/3d electrons in bonding synergistically to enhance OER activity.

The authors concluded that the special double perovskite structure with multiple metal-active sites, three-dimensional ordering and a corner (or edge)-sharing network *via* O atoms is well suited to maximize synergistic effects and is expected to break through the limit of the OER bottleneck for water splitting. (Reported by Ashish Chainani)

*This report features the work of Zhiwei Hu, Jian-Qiang Wang, Linjuan Zhang and their collaborators published in Adv. Functional Mater. 31, 2104746 (2021).*

### TPS 44A Quick Scanning X-ray Absorption Spectroscopy

#### TLS 11A1 Dragon MCD, XAS

- XANES, EXAFS, XAS
- Materials Science, Chemistry, Condensed-matter Physics

### References

1. L. Li, H. Sun, Z. Hu, J. Zhou, Y.-C. Huang, H. Huang, S. Song, C.-W. Pao, Y.-C. Chang, A. C. Komarek, H.-J. Lin, C.-T. Chen, C.-L. Dong, J.-Q. Wang, L. Zhang, Adv. Functional Mater. **31**, 21047746 (2021).
2. J.-H. Choy, D.-K. Kim, S.-H. Hwang, G. Demazeau, D.-Y. Jung, JACS **117**, 8557 (1995).